Equilibrium effects on the structure of magnetic islands and its impact on the plasma transport

S. Zhou[1, 2], Y. Liang[1, 2], Y. Suzuki[3], Z. S. Wang[2], J. Yang[2], A. Knieps[1], Z. Huang[1, 2], N. C. Wang[2], B. Rao[2], Y. H. Ding[2] and the J-TEXT team[2]

[1] *Institute of Energy and Climate Research, Plasma Physics IEK-4 Forschungszentrum Jülich GmbH, Jülich, Germany*

[2] *International Joint Research Laboratory of Magnetic Confinement Fusion and Plasma Physics, Huazhong University of Science and Technology, Wuhan, China*

[3] *National Institute for Fusion Science, Toki, Japan*

Equilibrium effects on the structure of magnetic islands is an important and fundamental research in magnetically confined fusion devices [1]. Here, the equilibrium effect is defined as the plasma self-consistent responses to the change of the magnetic topology, and it is an equilibrium solution of the interactions between the plasma with a finite pressure gradient and magnetic fields induced by the external coils and the plasma current. In tokamak plasmas, the application of resonant magnetic perturbations (RMP) could break the initial axisymmetry and change the magnetic topology. To understand the plasma equilibrium response to the RMP fields, fully 3D non-linear magnetohydrodynamics (MHD) equilibrium calculations have been carried out using the HINT [2] code on J-TEXT tokamak [3]. It turns out that the equilibrium effects can significantly change the structure of the magnetic islands, which in turn impacts the plasma transport.

RMP field penetration experiment on J-TEXT

In this experiment, the target plasma with R = 1.05 m, a = 25.5 cm, a toroidal magnetic field B_t = 2 T at magnetic axis and a toroidal current I_p = 175 kA was sustained stably for 400 ms from t = 0.2 s to t = 0.6 s with Ohmic heating. Figure 1 shows an overview of a typical discharge from the m/n = 2/1 field penetration experiment on J-TEXT. The m/n = 2/1 field penetration, followed with a sudden substantial degradation of plasma confinement, occurred at t = 0.27 s, when the I_{RMP} reached ~2.8 kA. The time evolutions of the central line-integrated electron density and SXR emission, and the plasma core electron temperature showed a sudden significant drop during the excitation of the m/n = 2/1 magnetic island. All profiles partially recovered after the RMP coil current was turned off. Since the density feedback control system was turned off in this experiment, the electron density did not fully recover, and the electron temperature was even slightly higher.

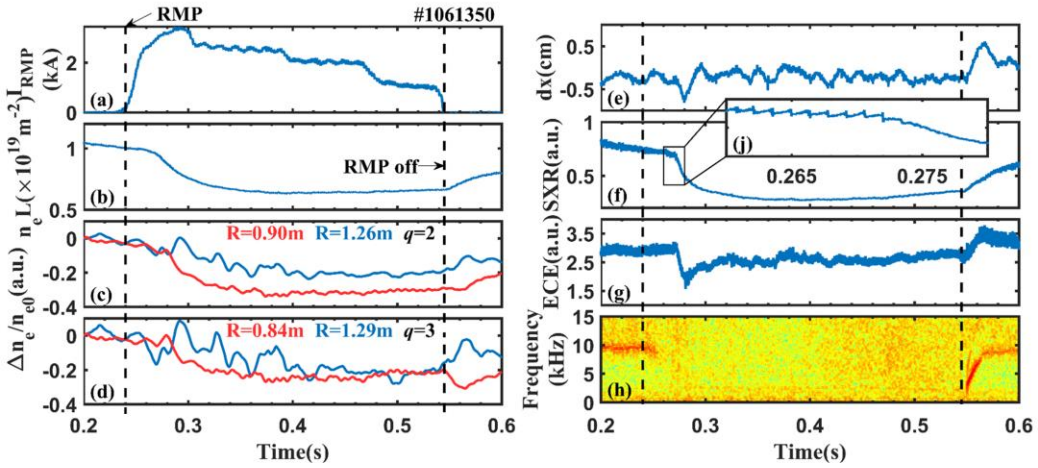

Figure 1. Overview of the RMP m/n=2/1 field penetration discharge #1061350 on J-TEXT. (a) The RMP current, (b) the central line-integrated electron density, (c) the normalized electron density at $q = 2$ region ($\Delta n_e = n_e - n_{e0}$ and n_{e0} is taken at $t = 0.2$ s), (d) the normalized electron density at $q = 3$ region, (e) the horizontal displacement, (f) the intensity of the core chord-integrated SXR emission, (g) the relative electron temperature from ECE at minor radius r =16.87 cm, (h) the magnetic spectrum of the Mirnov signal.

3D magnetic topology vs. the local measurements of plasma profiles

The plasma equilibrium for the discharge shown in figure 1 was calculated using the 3D MHD equilibrium code HINT. Figure 2 shows the correlation between the magnetic structure at the horizontal plane $Z = 0$ calculated by the HINT code, and the time evolution of the electron temperature profile measured by the ECE diagnostic. According to 3D equilibrium calculation results as shown in figure 2(a), the O-point of the $m/n = 2/1$ magnetic islands at the low-field side is located at $\phi = 180°$, while the view-port of the ECE diagnostic is located at $\phi = 225°$. Figure 2(b) shows an obvious change in electron temperature appearing near the $q = 2$ flux surface after the RMP field penetration occurs, and a higher amplitude of the RMP coil current apparently results in a larger temperature reduction and a wider region of $T_e/T_{e0} < 1$.

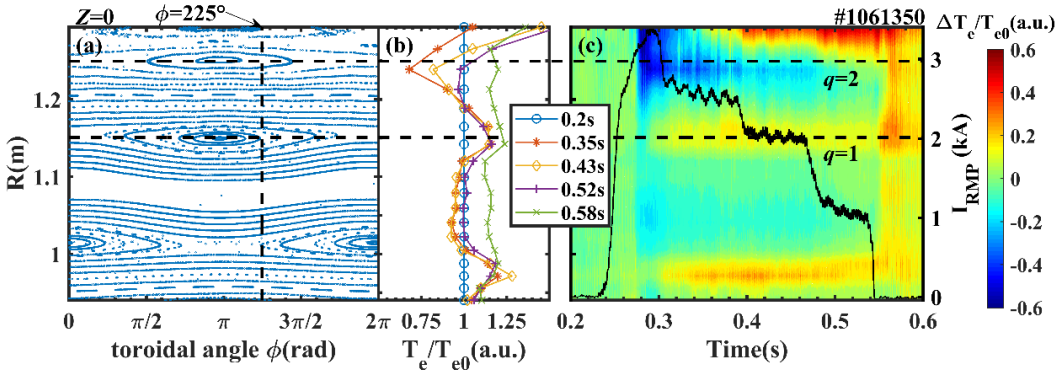

Figure 2. Magnetic topology calculated at horizontal plane $Z = 0$ and measured electron temperature profiles ($\Delta T_e = T_e - T_{e0}$ and T_{e0} is taken at $t = 0.2$ s). (a) Poincaré plot, (b) normalized electron temperature profiles measured at five times, (c) contour plot of normalized electron temperature. The black solid line in (c) is the RMP coil current.

The Poincaré plots and connection length distributions of magnetic topologies calculated by vacuum model and HINT at $\phi = 0°$ for $I_{RMP} = 3$ kA are given in figure 3. Compared with the HINT calculation, the $m/n = 1/1$ magnetic island is larger and the stochastic effect at the edge region is more pronounced for the vacuum model. In addition, some sideband mode structures are more obvious in the HINT model (e.g. the $m/n = 3/2$ magnetic island). The X-points of the $m/n = 2/1$ and 3/1 islands show the highest differences (marked with rectangles in figure 3(a) and (b)). For the connection length distribution, the vacuum model (figure 3(c)) illustrates that there are more magnetic field lines with connection length below 2000 m, indicating that the stochastization effect is more significant in the vacuum model. Even at $r \sim 0.22$ m, there are quite a few open field lines. In the HINT calculation (figure 3(d)), the stochastization effect is reduced, and the region where the field line connection length remains infinity becomes larger, suggesting a better edge confinement in the HINT results compared to the vacuum model.

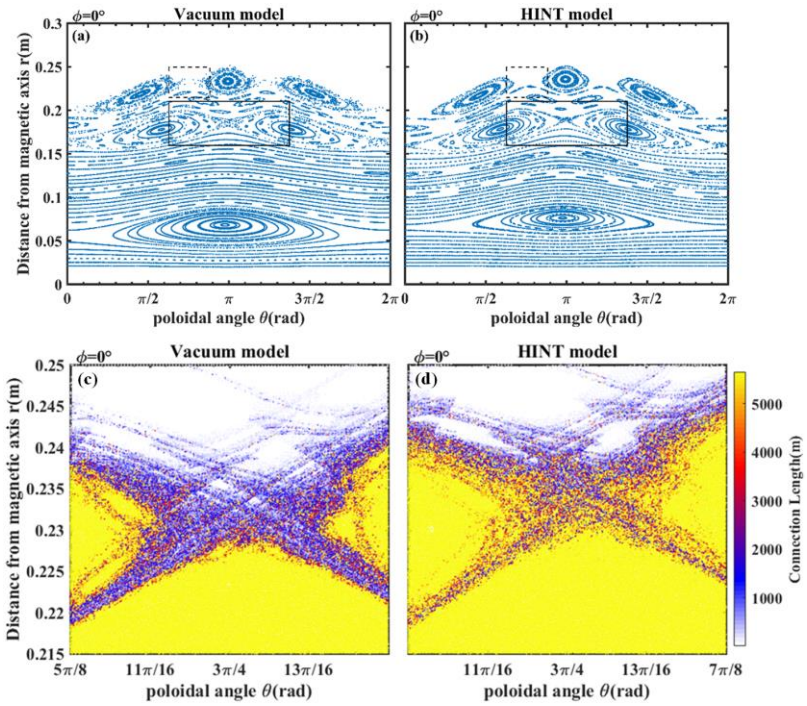

Figure 3. Poincaré plots and connection length distribution of the vacuum approximation model and HINT model at $\phi = 0°$ for $I_{RMP} = 3$ kA. The top two figures are the Poincaré plots, (a) Vacuum model and (b) HINT model. The solid rectangle marks an X-point of the 2/1 magnetic island chain and the dashed rectangle marks an X-point of 3/1 magnetic island chain. The bottom two figures are connection length distributions around X-point of the 3/1 magnetic island chain, (c) Vacuum model and (d) HINT model.

Edge magnetic island effects on the plasma transport

In order to investigate the effects of edge magnetic island on the plasma transport, $m/n = 3/1$ RMP configurations (different from the above 2/1 field penetration experiment (figure 1-3)) and the edge reciprocating Langmuir probe (RLP) have been applied. Figure 4 shows the

Poincaré plots calculated by HINT and edge plasma profiles measured by RLP for two different RMP phases, including #1056901 with the RLP near O-point of 3/1 island (shown in figure 4(a)) and #1056900 near the X-point correspondingly (shown in figure 4(b)). The electron pressure profiles (P_e, figure 4(c)) indicate that there exists a flattening region near the O-point of 3/1 island and a steep pressure gradient near the X-point of 3/1 island. The radial electric field (E_r, figure 4(d)) is charged much more positive near the O-point of 3/1 island than near the X-point. Figure 4(e) and (f) show the radial particle transport (Γ_r) driven by turbulence. It indicates that larger Γ_r can be obtained near the X-point of 3/1 island rather than O-point.

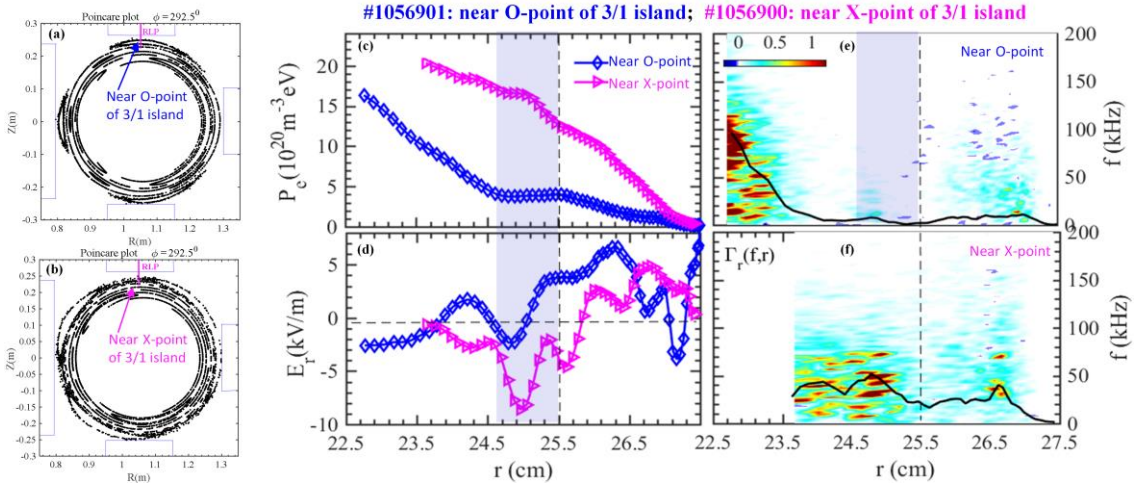

Figure 4. Poincaré plots and edge plasma profiles for two different RMP phases. The two Poincaré plots show that (a) the RLP near X-point of 3/1 island and (b) near the O-point. The edge plasma profiles are measured by the RLP, including (c) electron pressure, (d) radial electric field, (e) and (f) radial particle transport driven by turbulence.

Conclusions and outlook

Based on the 3D equilibrium simulations, the structure of magnetic islands changed by the equilibrium effects can differ significantly from the simple vacuum assumption. From the measurements of edge plasma profiles, it demonstrates that turbulence transport can be strongly modified by the magnetic island structure. It is currently unclear how the MHD-driven changes interact with the screening effect of plasma rotation, which was neglected in this analysis.

Acknowledgments

This work was supported by the National Key R&D Program of China (No. 2018YFE0309100), and by National Natural Science Foundation of China (No. 51821005).

References

[1] Suzuki Y 2017 Plasma Phys. Control. Fusion 59 054008

[2] Suzuki Y et al 2006 Nucl. Fusion 46 L19

[3] Liang Y et al 2019 Nucl. Fusion 59 112016